Asociación Argentina
de Mecánica Computacional

Mecánica Computacional Vol XXVII, págs. 2715-2732 (artículo completo)
Alberto Cardona, Mario Storti, Carlos Zuppa. (Eds.)
San Luis, Argentina, 10-13 Noviembre 2008

DAMAGE DETECTION IN STRUCTURAL ELEMENTS TAKING INTO ACCOUNT A CRACK CONTACT MODEL

Fernando S. Buezas[a,b], Marta B. Rosales[b,c] and Carlos P. Filipich[c,d]

[a]*Dept. of Physics, Universidad Nacional del Sur, 8000 Bahía Blanca, Argentina, fbuezas@gmail.com.ar*
[b]*CONICET, Argentina*
[c]*Dept. of Engineering, Universidad Nacional del Sur, 8000 Bahía Blanca, Argentina, mrosales@criba.edu.ar*
[d]*Centro de Investigaciones de Mecánica Teórica y Aplicada, FRBB, Universidad Tecnolgica Nacional, 8000 Bahía Blanca, Argentina, cfilipich@yahoo.com.ar*

Keywords: crack detection, genetic algorithm, contact problem

Abstract. This paper deals with the crack detection in structural elements by means of a generic algorithm optimization method. Both beam-like structures and arbitrary shaped structural elements may be handled through bi- and three dimensional models. The crack model takes into account the existance of contact. Many of the methods to detect a crack in beam-like structures are based on linear one-dimensional models and are not straightforwardly applicable to structures such as beams or arcs with an open crack or a breathing crack without or with contact. The present study deals with bi- and three-dimensional models to handle the dynamics of a structural element with a transverse breathing crack. The methodology is not restricted to beam-like structures since it may be applied to any arbitrary shaped 3D element. The crack is simulated as a notch or a wedge with a unilateral *Signorini*'s contact model. The contact may be partial or total. All the simulations are carried out using the partial differential solver of the general purpose, finite element code FlexPDE. A genetic algorithm (GA) optimization method is successfully employed for the crack detection. The dynamic response at some points of the damaged structures are compared with the solution of the computational (FE) model using least squares for each proposed crack depth and location. An objective function arises which is then optimized to obtain an estimate of both parameters. Physical experiments were performed with a cantilever damaged beam and the resulting data used as input in the detection algorithm.

1 INTRODUCTION

The first research on the damage detection through vibration measurements were published before the experimental modal analysis. The computational power and the experimental capacity to data acquisition were very limited at that time, which may explain that the first detection methods reported in literature are only based on natural frequency changes. In the review by Doebling et al. (1998), Lifshitz is mentioned as the authors of the first published article using the vibration data to diagnosis the damage. From the data obtained parameters related with the value of the stress tensor were found as indicators of the damage. Back to the eighties finite elements started to be used as a computational tool to model damaged structural elements. Changes in the natural frequencies was the first and more studied criterium. Salawu (1997), Dimarogonas (1996), Owolabi and Seshadri (2003), Kim and Stubbs (2003) may be a reference on this research line. Khiema and Lienb (2004) employ these technique to detect many cracks. Some tries to detect the damage from the inverse problem were studies by Law and Lu (2005) and Rao and Rahman (2006). Anyway, the bad conditioning makes it difficult the detection as a pure inverse problem. Many works dealing with straigth beams has been reported. Wang and He (2007) use artificial neural networks (ANN) to detect crack in arc structural elements. The authors of the present work have employed ANN in beam-like structures and rotating beams (Rosales et al., 2006),(Rosales et al., 2008). The genetic algorithms appear as a good idea (Houck et al., 1995) to optimize an objective function that depends on the crack position and magnitude when a nonlinear dynamic is present, either due to large rotations or contact at the crack closing. Extensive work in this direction may be found in (Carneiro and Inman, 2000; Carlin and Garcia, 1996; Friswell et al., 1998). Contact at the crack can be modeled in many ways. Carneiro (2000) proposed a breathing crack model for a Timoshenko beam. These models have been employed in other areas of the Mechanica by Raous (1999); Kikuchi and Oden (1998). A thorough and detailed study of the mechanics of contact can be found in Johnson (1987). The structural models implemented in the present work are referred to the undeformed configuration or *Lagrangian* using the first and second Piola-Kirchoff tensor (Lai et al., 1993; Eringen, 1980; Truesdell and Noll, 2003).

The present study deals with bi- and three-dimensional models to handle the dynamics of a structural element with a transverse breathing crack. The methodology is not restricted to beam-like structures since it may be applied to any arbitrary shaped 3D element. The crack is simulated as a notch or a wedge with a unilateral *Signorini*'s contact model. The contact may be partial or total. All the simulations are carried out using the partial differential solver of the general purpose, finite element code FlexPDE.

A genetic algorithm (GA) optimization method is successfully employed for the crack detection. The dynamic response at some points of the damaged structures are compared with the solution of the computational (FE) model using least squares for each proposed crack depth and location. An objective function arises which is then optimized to obtain an estimate of both parameters. The optimization algorithm is developed within the MatLab environment and interacts with the FEM model. It was found that the functions present a large number of local minima. Given such a complexity, the standard optimization techniques (e.g. gradient methods) are not successful when used directly. Here the GA shows very acceptable behavior. Extensive studies were carried out to analyze the influence of the various parameters involved in the GA. The parametric studies allowed to set the optimal values for this problem like population, reproduction (heuristic crossover), number of generations, etc.

Large number of cases regarding crack detection in beam-like structures have been analyzed

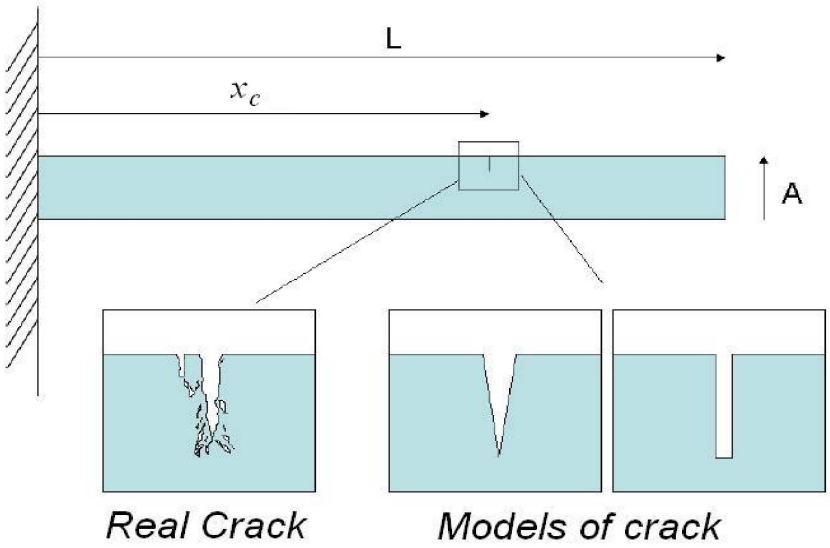

Figure 1: Real crack and the detection model.

within the present study. Physical experiments were performed with a cantilever damaged beam and the resulting data used as input in the detection algorithm. Both lineal and non-linear models were considered for the material. Here the first one is employed since the initial conditions given to the structural element in order to start the motion yield small deformations. The results were confirmed with the non-linear model. A general isotropic linear constitutive relationship between the second Piola-Kirchoff stress tensor and the Green-St. Venant strain tensor was proposed for the non-linear case. Additionally and when dealing with numerical experiments, a white noise was introduced and it was found that the errors remains in the same range. As the procedure is not restricted to beam-like elements other geometries were tackled, e.g. an arc (curved beam) and a blade-like structural element. Crack detection results on the latter are also reported. The methodology allows up to a third level detection, i.e. detection of damage existence, location and depth. The errors are reasonable given the nonlinearities introduced by the contact problem and the inherent complexity of the inverse problem.

2 STATEMENT OF THE PROBLEM

The crack detection will be performed on structural elements that will be tackled with two and three dimensional finite element models. In what follows a brief introduction on the governing equations within the Solid Mechanics field will be stated. Also the contact issue at the crack interface will be described. The beam problem (Figure 1) is the structural element more extensively studied since it allows for adjustments and validation but any arbitrary shaped structure(2D or 3D) could be handled. To show this fact, the crack detection in a blade-shaped element is included as an illustration.

2.1 Equations of Motion

The statement of the governing equations is made withing the frame of the Mechanics of Continuum with a *lagrangian* or material reference showing some advantages with respect to the spatial or *eulerian* reference for Solid Mechanics problems. For instance, if the continuum problem is given in the *eulerian* reference, besides the equations of motion (Cauchy equations)

(using direct notation)

$$\nabla \cdot \sigma + \rho \mathbf{b} = \rho \mathbf{a} \tag{1}$$

the mass continuity should be guaranteed,

$$\frac{d\rho}{dt} + \rho \nabla \cdot \mathbf{v} = 0 \tag{2}$$

where σ is the Cauchy stress tensor, ρ is the mass density, $\mathbf{b}$ are the body forces and $\mathbf{a}$ and $\mathbf{v}$ are the acceleration and velocity fields respectively. It should be noted that both $\mathbf{a}$ and $\mathbf{v}$ and $\frac{d\rho}{dt}$ are found as material derivatives, which impose a strong nonlinearity to the differential equations. For instance, $\frac{d\rho}{dt} = \frac{\partial \rho}{\partial t} + v \cdot \nabla \rho$. This is not the main drawback since if the body undergoes spatial finite displacements, the statement of the boundary equations is a mathematically inconsistent problem given that the position itself is one of the unknowns. However quasi-static update techniques applied to the boundary position regularize the problem. Now, if a *lagrangian* reference is used, only the motion problem should be solved,

$$\nabla \cdot \mathbf{P} + \rho_0 \mathbf{b} = \rho_0 \mathbf{A} \tag{3}$$

where $\mathbf{P}$ is the Piola - Kirchoff stress tensor, $\rho_0 = \rho(X, t_0)$ is the initial density (which is known) and $\mathbf{A} = \frac{\partial \mathbf{V}}{\partial t} = \frac{\partial^2 \mathbf{R}}{\partial t^2}$ (R is the position vector) is the acceleration field, that is simply the partial derivative of the velocity field.

The boundary conditions are imposed to the initial boundary (its position is known), leaving the statement of the boundary problem, the initial conditions and the equations of motion consistently closed. The position of any point of the body, including the boundary, will be known once the differential problem is solved. The nonlinear part is transferred to the tensor $\mathbf{P}$. This tensor is non-symmetric and its physical interpretation is not straightforward. The second Piola - Kirchoff tensor is symmetric and given by $\mathbf{P} = \mathbf{FS}$ where $[\mathbf{F}]_{ij} = \partial u_i / \partial X_j$ is the deformation gradient tensor, u_i is the $i-th$ component of the displacement vector $\mathbf{u}(\mathbf{X},t) = \mathbf{x}(\mathbf{X},t) - \mathbf{X}$, X_j is the $j-th$ component of the material field $\mathbf{X}$ and $\mathbf{x}$ is the position vector (spatial field). Thus the equations of motion are written as

$$\nabla \cdot (\mathbf{FS}) + \rho_0 \mathbf{b} = \rho_0 \mathbf{A}. \tag{4}$$

We need to relate $\mathbf{S}$ with the motion to round the differential problem that has vector $\mathbf{u}$ as unknown. Both tensor $\mathbf{P}$ and $\mathbf{S}$ are related to the Cauchy tensor σ. Here a very simple constitutive equation is proposed,

$$\mathbf{S} = \lambda \, tr(\mathbf{E}) \mathbf{I} + 2\gamma \mathbf{E} \tag{5}$$

where λ and γ are constants and $\mathbf{E}$ is the Green's strain tensor. Equation (5) is known as St. Venant–Kirchhoff material model (Truesdell and Noll, 2003) that, as is obvious, tends to Hooke's law for infinitesimal displacements, elastic homogenous and isotropic bodies (if $\mathbf{E} \rightarrow \varepsilon$ then $\mathbf{S} \rightarrow \sigma = \lambda \, tr(\varepsilon)\mathbf{I} + 2\gamma\varepsilon$) and λ and μ Lamé constants $\lambda = \nu E/(1+\nu)(1-2\nu)$, $\gamma = E/2(1+\nu)$, ν is the Poisson's coefficient and E the modulus of elasticity. $\varepsilon_{ij} = \frac{1}{2}\left(\frac{\partial u_i}{\partial x_j} + \frac{\partial u_j}{\partial x_i}\right)$ is the infinitesimal deformation tensor.

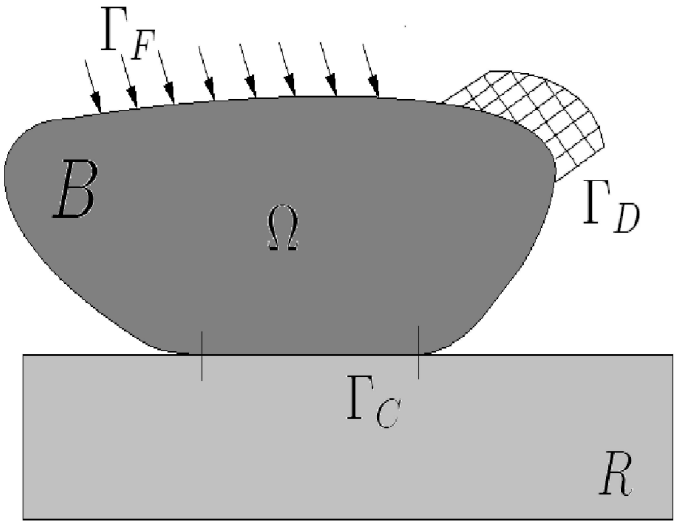

Figure 2: Scheme of contact between a deformable body and a rigid obstacle.

3 CONTACT MODELS

In this section a unilateral contact model between bodies undergoing arbitrary deformations. This type of problems presents large difficulties on the one hand due to the nonlinearities and on the other due to the difficulty of stating and solving a no holonomic restrictions problem, as is the present one. The regularization to a holonomic problem overcomes the obstacle and makes the way to more complex models that include friction, adhesion, etc.

3.1 Real contact surface

The real contact surface between two bodies is of the partial type between the roughness of both bodies. As the interpressure increases, the borders irregularities deform thus increasing the contact area. Not only the mechanical issue is present in the contact but also chemical reactions, electrical and thermal effects are present though not enough understood yet. In the present study the authors do not go deeper in the physical and chemical tribology issues.

3.2 Unilateral contact

As a first approach to the contact model let us supose that a deformable body interacts with a rigid and fixed obstacle. The contact condition is the no penetration of the body in the rigid obstacle.

3.2.1 Signorini problem

Let a body B with domain Ω in the space (or in a plane). B has a sufficiently smooth boundary $\Gamma = \Gamma_F \cup \Gamma_D \cup \Gamma_C$ which is sufficiently smooth which is in contact with other body R that is rigid and fixed in the plane, (if it is plane). The part Γ_F of the boundary Γ corresponds to the boundary where the stresses are prescribed (natural conditions of the problem) (Eq. 3). Γ_D corresponds to the part of the boundary where the displacements are prescribes (geometric conditions) and Γ_C is the part in contact with the rigid body R (see Figure 2)

At the contact region Γ_c the displacements $\mathbf{u}$ and stresses $\mathbf{t}_c$ may be decomposed in normal

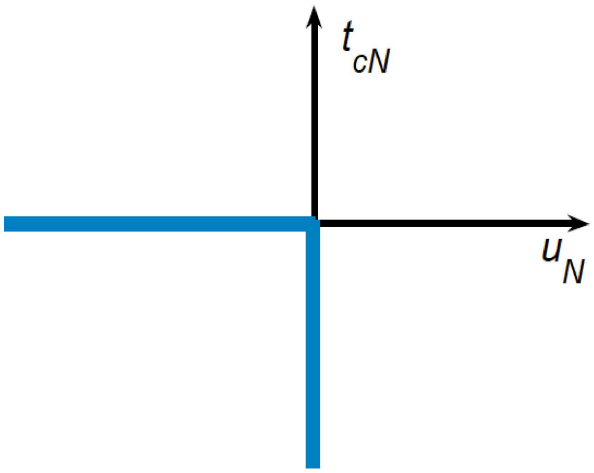

Figure 3: Signorini's law. t_{cN} is a multi-valued function of u_N at zero.

and tangential components in the following way

$$\mathbf{u} = u_N\,\mathbf{e}_n + u_T\,\mathbf{e}_t \tag{6}$$

$$\mathbf{t}_c = t_{cN}\,\mathbf{e}_n + t_{cT}\,\mathbf{e}_t \tag{7}$$

The Signorini problem (unilateral contact) is (see Figure 3)

$$\left.\begin{array}{c} u_N \leq 0 \\ t_{cN} \leq 0 \\ u_N\, t_{cN} = 0 \end{array}\right\} \tag{8}$$

It is easy observed that the Signorini conditions 8 are satisfied only with one of the following possibilites

1. No contact $\Rightarrow u_N \leq 0$ y $t_{cN} = 0$
2. Contact $\Rightarrow u_N = 0$ y $t_{cN} \leq 0$

The conditions (Eq. 8) form a non-continuous or non-smooth problem since t_{cN} is a multi-valued application of the field u_N (or simply t_{cN} is not function of u_N). From the Analytical Mechanics viewpoint the Signorini conditions form a non-holonomic constraints given by inequalities. This is apparent in the fact that neither the stresses nor the contact surface itself are known before solving the problem. If this were solved, the deformation could be calculated but they are necessary to the statement of the classical boundary problem. In other words, within the Continuum Mechanics the knowledge of the boundary conditions is mandatory to solve the problem, but on other hand the Signorini problem deals with the boundary conditions as unknown.

3.2.2 Extensions

Regarding the contact between two deformable bodies of two part of the same body, the Signorini problem allows to easily solve the contact problem if the deformations and displacements are infinitesimal, by making a change of variable. Now the problem is double (one for

each body surface and in the present study, one for each crack interfase).

$$\left.\begin{array}{c} d(x_1, x_2) \leq 0 \\ t_{cN1} \leq 0 \\ x_1\, t_{cN1} = 0 \end{array}\right\} \tag{9}$$

$$\left.\begin{array}{c} d(x_2, x_1) \leq 0 \\ t_{cN2} \leq 0 \\ x_2\, t_{cN2} = 0 \end{array}\right\} \tag{10}$$

where $d(x_1, x_2)$ is the distance between the spacial points x_1 that corresponds to body 1 and x_2 that corresponds to body 2. The advantage in using infinitesimal displacements is that unit vectors $N_2 = -N_1$ and the pair of points x_1 and x_2 are known before solving the problem and are on the surface normal.

Instead, if the displacements or deformations were finite, there would be no knowledge regarding which pair of point would be in contact nor the corresponding unit normal vectors. The smallest distance between all pair of points (one of each body) should be calculated and also evaluate the unit normal vectors for such pair of points.

$$\left.\begin{array}{c} \min(d(x_1, x_2)) \leq 0 \\ t_{cN1} \leq 0 \\ x_1\, t_{cN1} = 0 \end{array}\right\} \tag{11}$$

$$\left.\begin{array}{c} \min(d(x_2, x_1)) \leq 0 \\ t_{cN2} \leq 0 \\ x_2\, t_{cN2} = 0 \end{array}\right\} \tag{12}$$

3.2.3 Regularization of the non-holonomic Signorini problem

The contact law stated in the previous subsection is of holonomic type, since no regular equation given by an equality exists. Instead the contact problem poses a restriction given by a set of inequalities. Furthermore, when contact takes place, the stress value is not defined and, when there is no contact, the displacement value is not defined. This intermittency between a natural type condition and other of geometric type is what gives the non-regular character to the contact problem since the moment when the condition shifts from one to other state is an unknown of the problem.

The regularization idea consists in replacing the rigid condition by a smooth or regular one. The holonomic restriction problem is replaced by a non-constraints problem. The boundary condition will always be natural with the imposition of a functional relationship between stresses and displacements.

$$t_{cN} = \left\{ \begin{array}{cc} -k\,(u_N)^m & if \;\; u_N > 0 \\ 0 & elsewhere \end{array}\right. \tag{13}$$

where k is a number that, if sufficiently large, the problem given by Eq. 13 will approximate to Eq. 8 (see Figure 4)

4 OPTIMIZATION PROBLEM APPLIED TO THE CRACK DETECTION

First the optimization problem is stated. Then the genetic algorithm is briefly described and the studies carried out to adjust the procedure are described.

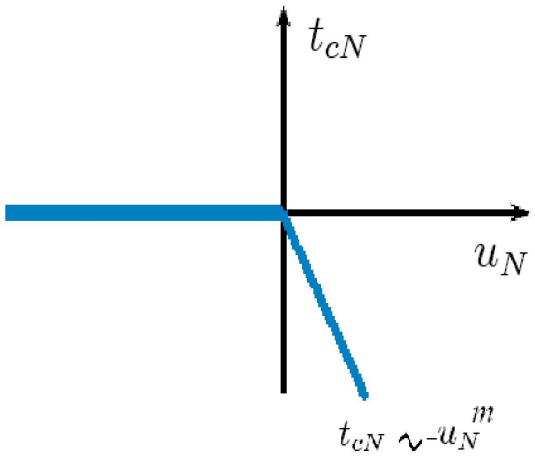

Figure 4: Regularization of Signorini's law. t_{cN} is continuous function of u_N at zero.

4.1 Optimization

The optimization of the inverse problem is attained through a least square criterium, i.e. the dynamic responses obtained from the experimental model are compared with the solution of a computational FEM model at certain points of the structure. The measurements are made at few points (no more than five). The detection problem consists in reconstructing the dynamic with this scarse information in order to solve the inverse problem by introducing the motion data and having the shape of the crack boundary as unknown (in the present study characterized by two parameters, crack depth —h_c— and location —X_c). Figure 5 shows an scheme of the dynamic experiment in which a perturbation introduced by hitting a hammer originates the transverse motion (though any type of motion could be studied). In the figure three sensors are shown, e.g. accelerometers, at three different locations. Finally an acquisitor completes the set up to obtain the data which yields the time functions $u(x_i, t)$ with $i = 1, \cdots, n$ ($n = 3$ in Figure 5).

On the other hand a computational model with a crack of parameters X_c and h_c of arbitrary values and displacements $u*(x_i, t)$ at the same points in which the accelerometers were located in the physical experiments. The comparison is then made between the two functions $u(x_i, t)$ and $u*(x_i, t)$. The objective function to be optimized in this study is

$$d(X_c, h_c) = \frac{1}{t_2 - t_1} \int_{t_1}^{t_2} \sum_{i=1}^{n} \left[u*(x_i, t) - u(x_i, t)\right]^2 dt \tag{14}$$

It was found that this objective function exhibits a large number of local minima. For such a complexity the usual optimization techniques based on gradient methods are not always successful. Then an approach based in a genetic algorithm is employed to perform the optimization.

4.2 The genetic algorithm (GA) approach

The GA method to solve optimization problems based upon the natural selection is inspired by evolutionary biology. A population of possible solutions of an optimization problem is generated by this technique. Each of these solutions is named *individual*. The individuals which

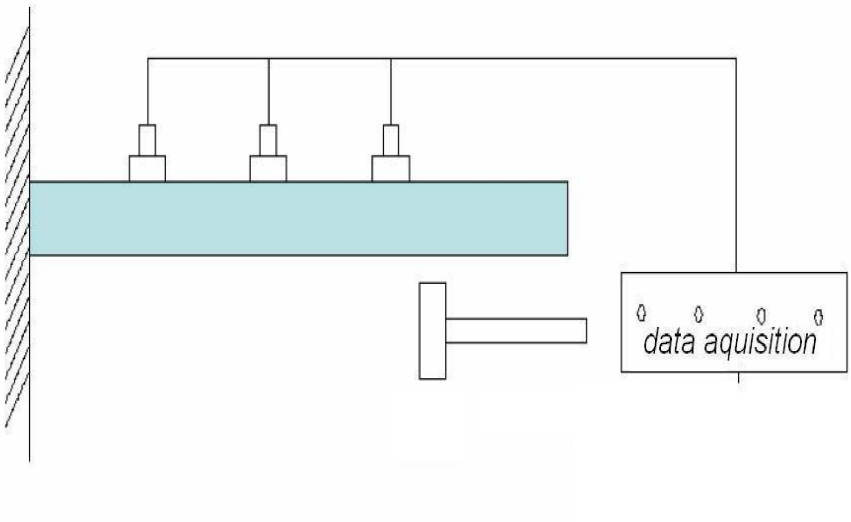

Figure 5: Scheme of experimental setup to detect the crack in a cantilever beam.

are closer to the real solution (i.e. the fitter) will be more capable to pass their (genetic) information to the next generation. In each generation the *population* evolves towards the optimal solution of the problem and the (genetic) information that passes from generation to generation will change according to the following rules:

Selection rule : a selection of the individual named *parent* is made following certain criterium that contributes to the next generation population.

Crossing rule : two parents are combined to create *children* for the next generation.

Mutation rule : random changes are introduced on the parents individuals that ensure the (genetic) diversity.

In particular, in the crack detection problem a set of values $J = (X_{cJ}, h_{cJ})$ is given. Each pair is an individual and the population is the whole set. The GA starts generation a random initial population of individuals. At this stage it is relevant to guarantee the largest diversity of solutions. Then new populations are generated. The steps followed in the GA optimization approach are briefly described below. For more detailed information, related bibliography may be consulted e.g. Houck et al. (1995), Carneiro (2000),Matlab (2006).

1. Evaluates each individual of the initial population (X_{cJ}, h_{cJ})
2. Orders the individuals giving them larger scores to the ones that yield a smaller $d(X_{cJ}, h_{cJ})$, i.e. better fitted.
3. Selects the individuals with larger scores (parents).
4. New individual are generated (children) through various ways: by means of random changes of a single parent (mutation) by combining the vector elements of a pair of individuals (crossing) or by identically repeating a child from a parent.
5. The parents population is replaced by the children (new generation).

Case	1	2	3	4	5	6	7	8	9	10
Crack location X_c	0.1	0.3	0.5	0.7	0.9	1.1	1.3	1.5	1.7	2
Crack depth h_c	0.1	0.1	0.2	0.2	0.1	0.2	0.1	0.2	0.1	0.2

Table 1: Simulated scenarios.

6. The genetic iteration ends when $d(X_{cJ}, h_{cJ})$ verifies some convergence criterium. Usually two criteria are employed (run the GA until a maximum number of times is reached or stop it no more changes are evident.

4.3 Adjustment of GA parameters

Different variables where tested to implement the GA algorithm in the crack detection problem by varying one parameter at a time and studying its optimum value. The parameters can be the simulation time, the number of sensors, the crack depth and location, and more specifically within the GA, the number of individuals, mutation parameters, maximm number of generations, crossing types. In the cracked beam problem an adjustment study was performed with the following example. A 2D elasticity finite element model is employed to study a clamped-free beam. The length is $L = 2.5$ m, the cross sectional area is $A = 0.25$ m^2, the elastic material has a modulus of elasticity $E = 7.310^{10}$ Pa, $\nu = 0.3$, mass density $\rho = 2766\ kg/m^3$. In this case the beam is assumed undamped. The dynamics is simulated and the response $u(X_n, t)$ is obtained with $n = 4$ simulating four sensors located at $X_n = nL/5$ that measure the transverse motion of the beam of Figure 5.

Regarding the parameters of the GA, the following are considered: uniform initial distribution, rank scaling, stochastic selection, elite count for the reproduction equal to 2 (this means that the two best individuals pass unaltered to the following generation), crossover fraction=0.8 (this corresponds to the 80% other than elite children) and scattered (the objective function is only dependent of two variables $d(X_c, h_c)$). The mutation is of the gaussian type and the stop criteria is a maximum number of ten generations and five repetitions for which the objective function does not improve. Graphics of the fitness function give clue of the necessary number of generations that are useful in the calculations. Among the parameters the crossing type was one of the studied. After various runs, it was concluded that the heuristic crossover with $r = 0.6$ was the optimum selection. In order to abstract statistical information of the parameter adjustments, ten scenarios are simulated (Table 1), using the heuristic crossover with $r = 0.6$ and now the number of individuals (population) is varied. A maximum number of five generations is adopted. The initial condition is a transverse velocity $v_y = -2x$ and the simulation time is 0.15 s.

The following non-dimensionalized error is computed

$$e_X = \frac{X_c - X_c^*}{L}; \qquad e_h = \frac{h_c - h_c^*}{A} \tag{15}$$

where X_c and h_c are the crack location and depth ; X_c^* y h_c^* are the crack location and depth that GA finds. The values e_x and e_h are the relative errors of the crack location and depth. The sum $e_r = |e_x| + |e_x|$ is the total error of each simulated scenario, which is a very strong measure. In order to establish the number of individuals necessary to attain acceptable results, the GA is run with different values of populations. The average errors are shown in percentage in Figure 6. The GA detects better the damage as the number of individual increases. An average total error less than 10 % is satisfactory.

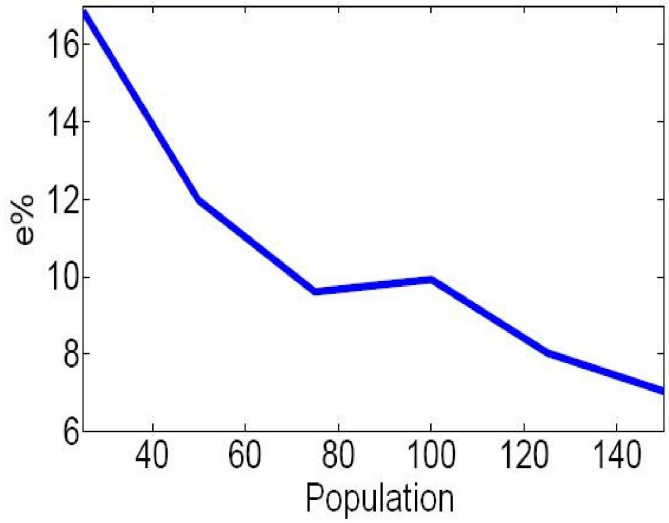

Figure 6: Influence of the population value.

Relative noise	0.1	0.2	0.3
Average error %	6.28	7.71	5.39

Table 2: Noise influence. Average errors.

In order to asses how long should be the experiment, the GA is run for a population of 50 individuals changing the simulation times. The percentage errors averaged are depicted in Figure 7.

The GA is not as efficient to detect the damage as the simulation time increases. The reason is that the objetive function $d(x_c, h_c)$ exhibits a larger number of local minima as the simulation time increases. Consequently, if a detection is desired in the case of a response of large duration, larger populations should be employed. An empirical rule adopted in the present study is to take 50 individuals por each one and a half fundamental period of the undamaged specimen.

4.4 Noise influence

Up to this stage crack detection problems on a beam with a simulated dynamic were dealt with. No uncertainties are included in the model neither the unavoidable experimental errors. With the aim of studying the robustness of the proposed methodology to more realistic signals, a white noise is incorporated to the signal of the simulated dynamic, keeping the population (50) and simulation time ($0.05s$, one and a half period of the healthy beam approximately)

Each of the noise signals have a relative magnitud of 0.1, 0.2 and 0.3 relative to the original signal and 1, 2 and 3 with respect to the first sensor. Table 4.4 depicts the average errors calculated by the sum of 15 for the same ten scenarios. The robustness of the detection method to this levels is noise may be observed.

4.5 Diffuse crack

The encouraging result from the previous subsection gives the way to the treatment of systems with inclusion of model uncertainties. A very exact computational model that simulates realistically the dynamics of a cracked body is available. But notwithstanding the detailed mod-

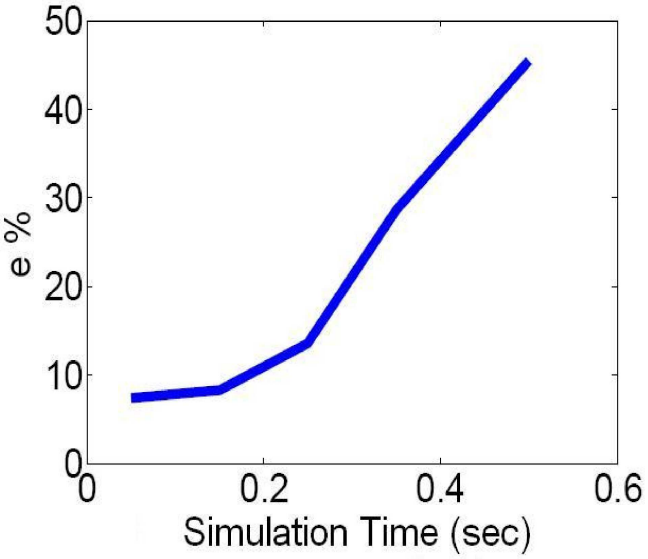

Figure 7: Influence of the simulation time. Population of 50 individuals.

caso	(Error %)	Case to detect		Detected by GA	
		x_c	h_c	x_c^*	h_c^*
1	7.161	0.3	0.1	0.32	0.115
2	8.124	0.7	0.1	0.55	0.105
3	4.647	1.3	0.2	1.25	0.206
4	6,724	1.5	0.2	1.36	0.197
5	41.32	1.9	0.1	2.37	0.044
6	6.508	1	0.12	0.98	0.134

Table 3: Diffuse crack. Six studied cases.

eling, it still has simplifications. A real problem presents uncertainties in the physical model that are approximated with theoretical or computational models which will be more or less closer to the physical model. The question that arises is, what is happening when a detection is desired in a real specimen with a real crack using this scheme? Let us suppose that the real crack be arbitrary shaped as shown in the left lower part of Figure 1. Will it be possible to detect such crack if its model is given by the scheme shown in the right lower part of Figure 1?

To answer this question, the simulation of the cracked beam dynamics different from the single crack model. In particular a diffuse type (five cracks in a small region, Figure 8) is simulated as it were a real experiment of a real body and the model of a single crack used to make the detection. The parameters are the individual numbers (50) and the simulation time (0.05 s).

Table 3 contains the six studied cases. The errors are calculated as defined above (i.e. the sum of the relative errors of each crack parameter). Only the 5th. case can be considered a failure.

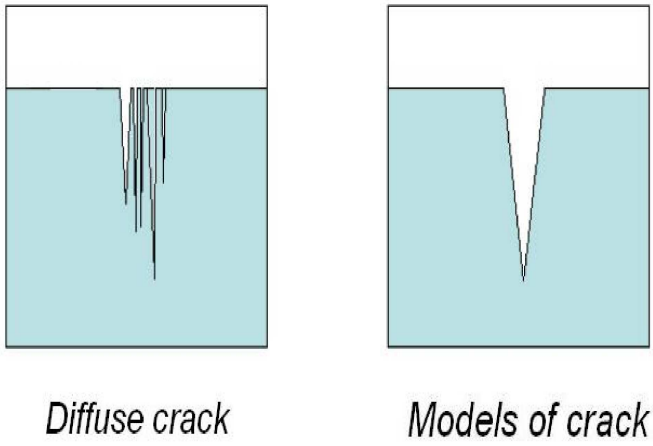

Figure 8: Diffuse crack models and detection model.

4.6 Experiment

Once the GA parameters and the simulation time have been chosen and accepting certain robustness in the crack shape and the experimental noise, the detection is performed in a real specimen. Two PASCO accelerometers are employed, each with mass $m = 34.7$g. The rod is made of aluminum, of length $L = 41.5\ cm$ (free length), square cross-section of side $a = 0.788\ cm$. The beam is clamped at a table and the accelerometers are located at $x_1 = 23.25$ cm and $x_2 = 34$ cm from the clamping. Since the model uncertainties are unavoidable, either in the boundary conditions, damping coefficients, elastic modulus or inhomogeneity of the material, a zero setting is carried out to homogenize the parameters in such way that the differences between the computational and physical models be a minimum. Using the GA algorithm the function

$$d(E, \mu_d) = \frac{1}{t_2 - t_1} \int_{t_1}^{t2} \sum_{i=1}^{2} \left[u^*(x_i, t) - u(x_i, t)\right]^2 dt \tag{16}$$

is minimized to find the following parameters: elastic modulus E y and the external damping coefficient μ_d (air friction), for a period $t_2 - t_1 = 0.1\ seg$. The GA algorithm were set with a population of 50 individuals, heuristic crossover up to 5 generations giving the following optimum parameters: $E = 36.567\ 10^9 Pa,\ \mu_d = 840.57$.

In order to reproduce in the physical test the same initial condition a weight of mass $m = 266.12$ g is hung from the free end of the beam. Then, to initiate the motion, the thread is cut with fire. Thus a minimum perturbation in the initial condition is ensures. The two motion sensors register the vibration motion of the undamaged beam in the acquisitor. Figure 9 shows the accelerations at points x_1 and x_2 for the experiment and 10, the ones corresponding to the simulation with the optimal parameters taking into account the masses and location of the accelerometers.

Certain similarity is observed in the acceleration amplitudes as well as the dissipation of the signals.

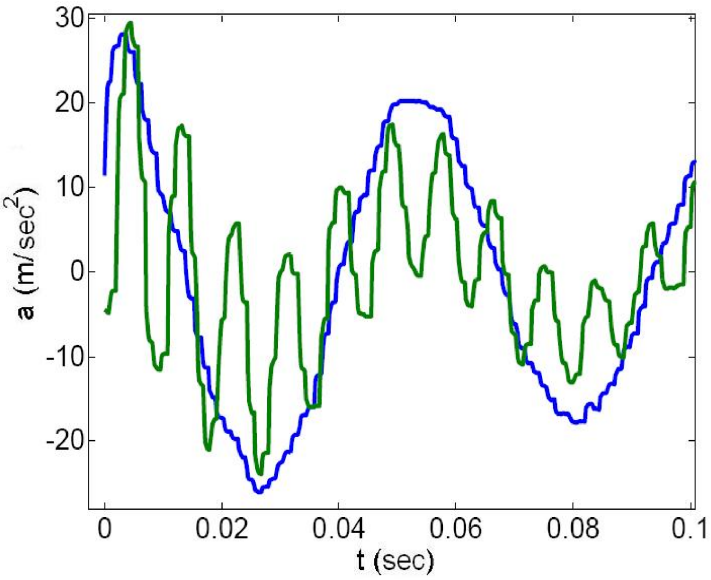

Figure 9: Acceleration at points x_1 (blue) and x_2 (green) for the undamaged beam. Physical model.

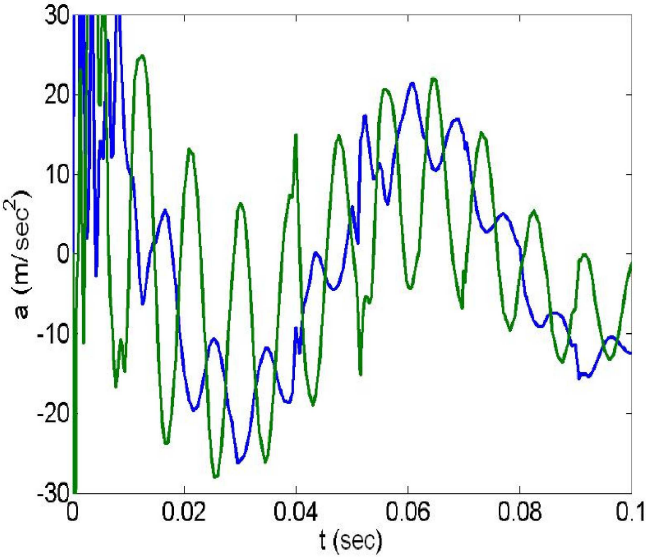

Figure 10: Acceleration at points x_1 (blue) and x_2 (green) for the undamaged beam. Computational model.

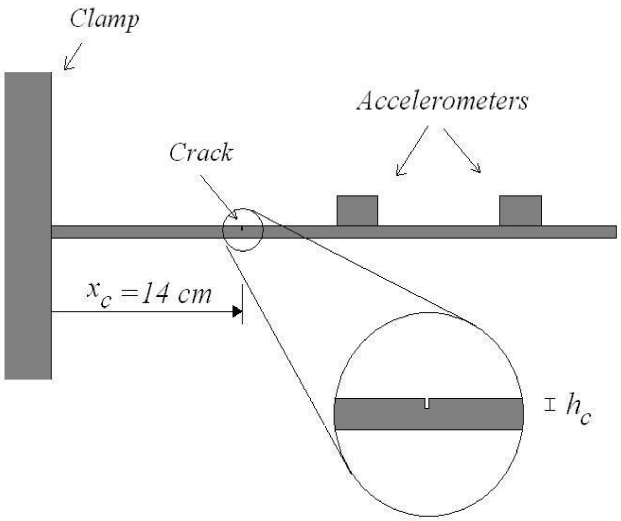

Figure 11: Scheme of the cracked aluminum beam.

Case	x_c/L	h_c/a	x_c/L detected	h_c/a detected
1	0.337	0.329	0.378	0.257
2	0.337	0.507	0.282	0.366
3	0.337	0.634	0.357	0.548

Table 4: Crack parameters detected with GA using a physical experiment.

To asses the damage in the beam and once the model is calibrated, notches are made with different depths: $2.6\ mm,\ 4\ mm\ y\ 5\ mm$ and of $1\ mm$ width, at $14\ cm$ from the clamping (see Figura 11).

Again, the optimization of $d(x_c, h_c)$ is made for the time $t_2 - t_1 = 0.1$ seg using $E = 36.567\ 10^9$ Pa,$\mu_d = 840.57$ with parameters: a population of 75 individuals, heuristic crossover with up to 5 generations.

This shows that the methodology may be employed to detect crack depth and position considering the opening and closure of the crack in a dynamic experiment of a damaged specimen. At this stage of the study, the experiment was performed which rather low precision instrumental, in order to design the methodology. Nevertheless, the results may be considered encouraging.

4.7 Crack detection in a blade-like element

Since the developed mechanical model is general regarding the type of motion (large deformations, rotations and displacements) and the geometry, 3D models of arbitrary shaped structural elements can be studied. Figure 12 depicts an scheme of a blade-like element that could resemble the blade of a wind turbine. The blade is made of steel and the geometry is generated by a plane that models the plane shape with a length $L = 8$ m and a maximum width of $a = 1.55$ m. The blade is very thin (0.08 m) and the warping along its length is given by $0.04 + 0.04\cdot$ and $\cdot(x-1) - 0.1 \cdot x$. The blade rotates 10 rad/seg around axis z and a simulation of almost a complete rotation is simulated with 0.5 s without including noise. The material model corresponding to steel is given by Eq. 5 where the Lamé constant correspond to steel and are found with $E = 2.05 \times 10^{11}\ Pa$ and $\nu = 0.3$. The GA parameters are: population 75,

Case	x_c/L	h_c/a	x_c/L detected	h_c/a detected	Error %
1	0.375	0.645 16	0.351 39	0.678 06	5.6 51
2	0.287 5	0.06 451 6	0.312 70	0.05 805 7	3.023

Table 5: Crack detection in a 3D blade-like element.

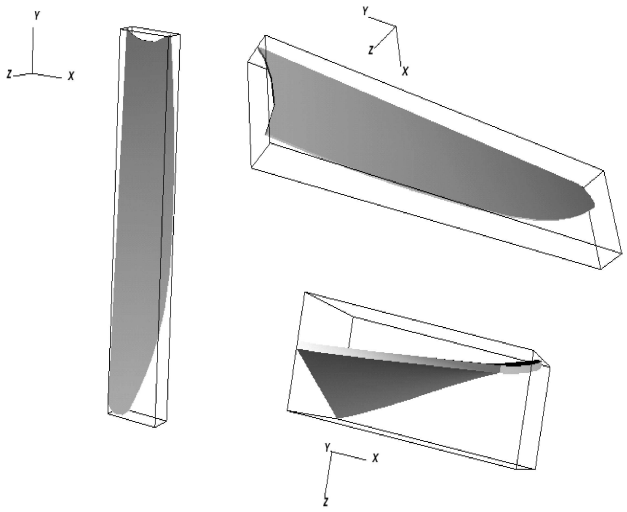

Figure 12: Views of the 3D blade-like structural element.

10 generations, heuristic crossover with$r = 0.6$. Case 1: $x_c = 3\ m;\ h_c = 1\ m$ and Case 2: $x_c = 2.3\ m;\ h_c = 0.1\ m$. The results are shown in the following table,

5 FINAL COMMENTS

A methodology based on genetic algorithms to be employed for the crack detection on damaged structural elements was presented. The technique proved to be successful in the studied cases and allows up to level three detection. The optimization is performed to an objective function constructed from the dynamics of the studied body. This dynamic is modeled within the Mechanics of Continuum with a *lagrangian* reference which offers important advantages when a contact model at the crack interfaces is desired. The breathing crack was idealized either by a straight notch or a wedge and following Signorini's contact theory of two bodies with finite deformations. Since arbitrary shaped bodies can be handled with the present nonlinear elasticity approach, different shape cracks, realistic contact simulations, arbitrary motions, arbitrary shaped structural elements can be tackled. First crack detection was perfomed using computational experiments and afterwards a physical experiment on a beam was employed to validate the methodology. Extensive computational studies were performed to calibrate and find the optimum GA parameter values and the damaged body dynamics. A relevant conclusion was that the number of individuals is directly proportional to the simulation time for long time periods. Additionally, the crack detection was applied to the a blade-like structural element through a 3D model. This element could be the representation of the a wind turbine blade, undergoing rotation. The nonlinear elasticity frame allows to extend the methodology to any arbitrary shaped body. The authors are at present studying the static analysis (with evident computational economies) and thermo-mechanic detection techniques.

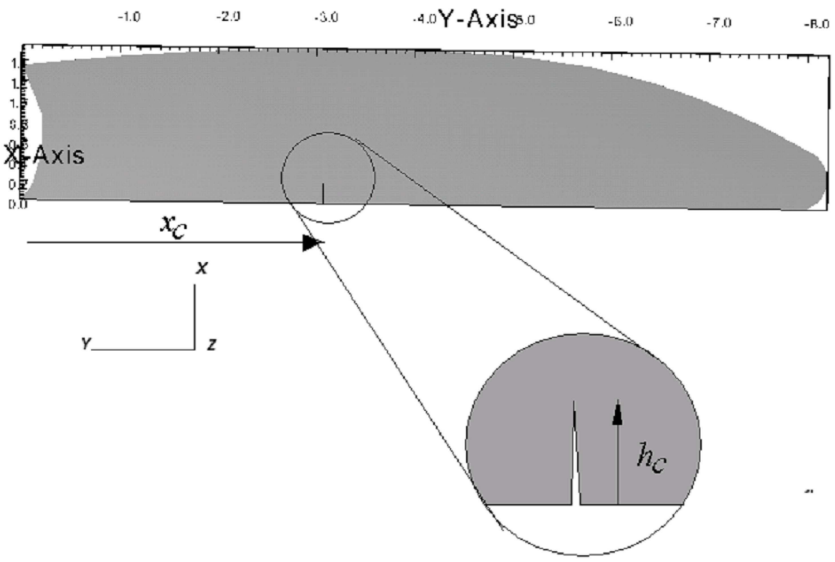

Figure 13: Cracked blade.

REFERENCES

R. A. Carlin and E. Garcia. Parameter optimization of a genetic algorithm for structural damage detection. In *International Modal Analysis Conference*, volume 18, pages 194–200, 1996.

S. H. S. Carneiro. *Model-Based Vibration Diagnostic of Cracked Beams in the Time Domain*. PhD thesis, Faculty of the Virginia Polytechnic Institute and State University, 2000.

S. H. S. Carneiro and D. J. Inman. A continuous model of a cracked timoshenko beam for damage detection. In *18th. Int. Modal Analysis Conference*, pages 194–200, 2000.

A.D. Dimarogonas. Vibration of cracked structures: state of the art review. *Engineering Fracture Mechanics*, 55:831–857, 1996.

S. W. Doebling, C. R. Farrar, and M. B. Prime. A summary review of vibration-based damage identification methods. *The Shock and Vibration Digest*, 32:2, 1998.

A. C. Eringen. *Mechanics of continua*, volume I. ROBERT E. KRIEGER Publ. Co., 1980.

M. Friswell, J. E. T. Penny, and S. D. Garvey. A combined genetic and eigensensitivity algorithm for the location of damage in structures. *Computational Mechanics*, 69:547–556, 1998.

C. R. Houck, J.A. Joines, and M. G. Kay. A genetic algorithm for function optimization: a matlab implementation. In *Tech. Rep. NCSU-IE*, volume 95, page 09, 1995.

K.L. Johnson. *Contact Mechanics*, volume I. Cambridge University Press, 1987.

N.T. Khiema and T.V. Lienb. Multi-crack detection for beam bythe natural frequencies. *Journal of Sound and Vibration*, 273:175–184, 2004.

N. Kikuchi and J.T. Oden. Contact problems in elasticity: a study of variational inequalities and finite element methods. *Studies in Applied Mathematics*, 273:175–184, 1998.

J.T. Kim and N. Stubbs. Crack detection in beam-type structures using frequency data. *Journal of Sound and Vibration*, 259:145–160, 2003.

W. M. Lai, D. Rubin, and E. Krempl. *Introduction to Continuum Mechanics*, volume I. Butterworth-Heinemann Ltd, 1993.

S.S. Law and Z.R. Lu. Crack identification in beam from dynamic responses. *Journal of Sound and Vibration*, 285:967–987, 2005.

Matlab. *Genetic Algorithm and Direct Search Toolbox 2.3*, 2006. V.7.

A.S.J. Owolabi, G.M.and Swamidas and R. Seshadri. Crack detection in beams using changes in frequencies and amplitudes of frequency response functions. *Journal of Sound and Vibration*, 265:1–22, 2003.

B. N. Rao and S. Rahman. A continuum shape sensitivity method for fracture analysis of isotropic functionally graded materials. *Computational Mechanics*, 38:133–150, 2006.

M. Raous. Quasistatic signorini problem with coulomb friction and coupling to adhesion. *New developments in contact problems Courses and Lectures*, 384:101–178, 1999.

M.B. Rosales, C.P. Filipich, and F.S. Buezas. Crack detection in beam-like structure. Under review, 2008.

M.B. Rosales, C.P. Filipich, and Buezas F.S. Crack detection in beam-like structures using a power series technique and artificial neural networks. In *In Proc.of the Thirteenth International Congress on Sound and Vibration (ICSV13)*, volume 18, pages 194–200, 2006.

O. S. Salawu. Detection of structural damage through changes in frequency: a review. *Engineering Structures*, 19:718–723, 1997.

C. Truesdell and W. Noll. *The Non-Linear Field Theories of Mechanics*, volume I. Springer-Verlag Berlin Heidelberg New York, 2003.

B.S. Wang and Z.C. He. Crack detection of arch dam using statistical neural network based on the reductions of natural frequencies. *Journal of Sound and Vibration*, 302:1037–1047, 2007.